PHYSICAL REVIEW B VOLUME 23, NUMBER 4 15 FEBRUARY 1981

Polarized low-energy-electron diffraction from W(100)

G.-C. Wang, R. J. Celotta, and D. T. Pierce
National Bureau of Standards, Washington, D. C. 20234
(Received 10 July 1980)

A set of polarized low-energy-electron diffraction (PLEED) data from a W(100) surface measured using a polarized electron beam is presented. The data include conventional LEED profiles $I(E,\theta)$ as well as $S(E,\theta)$ profiles which measure the spin dependence of the scattering. These profiles are obtained for specular beams at angles of incidence from 9°–24° and for five nonspecular beams at normal incidence. The potential usefulness of $S(E,\theta)$ profiles for structure determination is discussed and the use of PLEED for spin analysis is assessed.

I. INTRODUCTION

Low-energy-electron diffraction has been used extensively for studying surface-atom equilibrium positions on various single-crystal surfaces.[1] The recent development of a high-intensity polarized electron source[2] provides an additional means to probe surface equilibrium structures. To date there have been only limited polarized low-energy-electron diffraction (PLEED) measurements of two surfaces, W(100) (Refs. 3–5) and Au (110).[6] In this work we present a set of data suitable for comparison to the results of a dynamical calculation.

Spin-dependent scattering occurs because of the interaction between the incident electron's spin $\vec{s}$ and its orbital angular momentum $\vec{L}$ as it scatters from the atomic core. This spin-orbit interaction energy[7] is proportional to $(1/r)\ (dV/dr)\ \vec{L}\cdot\vec{s}$, where V is the scattering potential. The scattered intensity for electrons with spin aligned parallel, $I_\uparrow$, or antiparallel, $I_\downarrow$, to the angular momentum will be different. We measure the strength of the spin dependence of the scattering by

$$S(E,\theta)=\frac{1}{P_0}\frac{I_\uparrow(E,\theta)-I_\downarrow(E,\theta)}{I_\uparrow(E,\theta)+I_\downarrow(E,\theta)}, \tag{1}$$

where θ is the scattering angle. We account for the fact that the polarization of the incident beam P_0 is less than unity with the factor $1/P_0$. It is the spin-averaged LEED intensity $\frac{1}{2}[I_\uparrow+I_\downarrow]$ that is observed in conventional LEED experiments.

The scattered intensities of Eq. (1) can be written in a kinematic approximation as

$$I(E,\theta)_{\uparrow(\downarrow)}\propto I_0\sum_{i,j} f_{i,\uparrow(\downarrow)}(E,\theta)f^*_{j,\uparrow(\downarrow)}(E,\theta) \times\exp[i\vec{K}\cdot(\vec{r}_i-\vec{r}_j)], \tag{2}$$

where $\vec{K}=\vec{k}'-\vec{k}$ is the momentum transfer from incident momentum $\vec{k}$ to final momentum $\vec{k}'$. This expression can be easily extended to include thermal vibration.[8] The atomic scattering factor $f(E,\theta)_{\uparrow(\downarrow)}$ for electrons with spin aligned parallel (antiparallel) to the quantization axis given by $\vec{k}\times\vec{K}$ is understood to include direct and spin-flip scattering amplitudes. Note that in our experiment, which gives $S(E,\theta)$, we measure only differences in scattered intensities and do not measure changes in beam polarization on scattering. In the kinematic approximation, for the special case of a lattice of identical atoms, Eq. (1) becomes

$$S(E,\theta)=\frac{1}{P_0}\frac{|f_\uparrow(E,\theta)|^2-|f_\downarrow(E,\theta)|^2}{|f_\uparrow(E,\theta)|^2+|f_\downarrow(E,\theta)|^2} \tag{3}$$

and we see that the spin-dependent information is entirely in the atomic scattering factors and not in the interference function [the exponential in Eq. (2)] which gives rise to the diffraction conditions in LEED.[9] The interference function is a factor in both numerator and denominator of Eq. (1) and cancels out. In the kinematic picture, the normalized difference in the scattered intensity given by Eqs. (1) or (3) may be viewed as arising from two coincident arrays of atoms where the scattering potential in one array differs from that of the other due to the spin-orbit interaction. If the scattering is calculated in a partial wave analysis, twice as many phase shifts are required, that is, one for each spin direction.

In reality, the kinematic picture is inadequate because about half of the scattered intensity is due to multiple scattering[10] and Eq. (1) cannot be reduced to Eq. (3). The quantity S still depends on the atomic scattering factors, but because of multiple scattering, even in the case of a lattice of a single kind of atom, it depends also on the surface structure. In fact, it is possible to have a spin dependence due to multiple scattering where no spin dependence is expected from single scattering at the same energy and macroscopic scattering geometry. Thus, a dynamical theory is required to explain the spin dependence in polarized LEED.

Dynamical calculations[11,12] which include spin as a variable have shown that $S(E,\theta)$ profiles

are very sensitive to the assumed geometrical structure and diffraction conditions. These initial calculations motivated our experimental effort to obtain spin-dependent LEED data in order to test whether such measurements will be useful in surface structure determination. To the extent that the spin-dependent scattering can be reliably calculated, we expect that spin-polarized LEED will be a useful addition to spin-averaged LEED. One of the present difficulties in LEED studies is quantitatively comparing experimental and calculated curves. Experimental intensity profiles are broad due to strong electron-electron scattering, are convoluted with the instrument response function, and suffer from the difficulties of accurately normalizing to incident beam current. Sophisticated reliability-factor analyses[13] have been devised to make quantitative comparisons between experimental and calculated curves. Calculations[11] of S for a W(100) surface with and without a 10% surface contraction showed dramatic changes in S; peaks in S disappeared or changed sign and there were significant shifts in the zero crossings. This sharp structure, which is expected since S is intrinsically a difference function, should facilitate comparisons between theory and experiment. Moreover, since S includes a normalization to the scattered intensity, variations of incident intensity do not affect it. Also, as shown in Sec. IV, the measured S is to first order independent of the instrument response.

Because the spin dependence of the scattering depends on the gradient of the potential, it, in principle, contains additional information about the potential although this factor has not as yet been exploited. Also, as can be seen from the data presented in Sec. III, although there is not a general correlation between maxima in $S(E,\theta)$ and minima in $I(E,\theta)$ as expected for atomic scattering, large values of $S(E,\theta)$ often do occur near intensity minima. Thus, $S(E,\theta)$ data will test these regions, thereby complementing the $I(E,\theta)$ data.

In this paper we present the $S(E,\theta)$ profiles for the (00) beam over a wide range of incident angles and for five nonspecular beams at normal incidence from an unreconstructed W(100) (1×1) surface. It is our hope that this large set of PLEED data will stimulate dynamical PLEED calculations and provide a first test of the usefulness of PLEED in structure determination.

The outline of this paper is as follows: We will describe the experimental apparatus in the next section. In the third section we present the experimental data and compare them with other available data and calculations. The effect of the instrument response on $S(E,\theta)$ is discussed in Sec. IV, and the use of PLEED for spin analysis is discussed in Sec. V.

II. EXPERIMENTAL APPARATUS

The apparatus, which is shown schematically in Fig. 1, consists of a spin-polarized electron gun attached to a surface analysis chamber by a straight-through isolation valve. The surface analysis chamber contains a manipulator for positioning the target crystal, a cylindrical mirror analyzer for Auger spectroscopy, an ion gun for sputter cleaning samples, and a mass spectrometer for residual gas analysis. The commercial LEED optics Faraday cup assembly has been modified by replacing the conventional electron gun by the negative electron affinity GaAs polarized electron source.

A. Polarized electron source

A complete description of the polarized electron gun used for these experiments has been published elsewhere[14] and will only be briefly reviewed here. The polarized electrons are created by photoemission from GaAs irradiated with circularly polarized light. The intensity of the photoemitted electron beam remains constant but the direction of polarization can be modulated by varying the polarization of the light from left- to right-circularly polarized. In the experiments des-

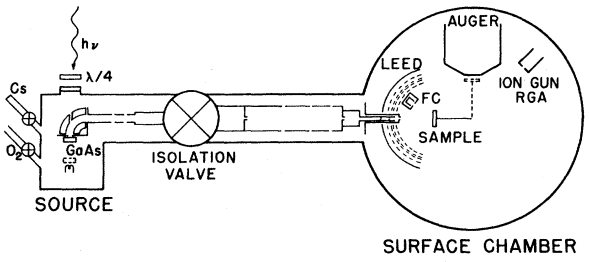

FIG. 1. Schematic of the PLEED apparatus. The GaAs spin-polarized electron source is separated from the surface analysis chamber by an isolation valve. The source contains provision for activating GaAs photocathode with Cs and O_2. The initial longitudinal polarization of the beam is changed to a transverse polarization (in the plane of the figure) by the 90° spherical deflector. A constant-intensity electron beam with modulated spin polarization impinges on the sample crystal in the surface chamber. The Faraday cup (FC) measures the modulation of the intensity of the scattered beam caused by a spin dependence of the scattering. To measure a spin-dependent signal due to the spin-orbit interaction, the Faraday cup must be out of the plane of the paper such that there is a component of incident spin polarization normal to the scattering plane.

cribed in this paper, the modulation of the circular polarization was obtained by rotating a quarter-wave plate or in later measurements by using a Pockels cell (an electro-optic modulator in which the optical retardation is proportional to the applied voltage).

The photocathode used in this work was a GaAs (100) wafer doped 5.6×10^{18} cm^{-3} p-type. It was chemically cleaned before insertion into the source chamber and then was cleaned in ultrahigh vacuum by heating. A negative electron affinity was obtained by applying Cs and O_2 to the GaAs surface. The incident light was produced by a GaAlAs diode laser and had an energy of 1.57 eV. With 0.5 mW incident on the GaAs a 10-μA emission current was obtained. The photocathode usually lasts for weeks without reactivation. The intensity decays to half its value in a day, but it can be readily returned to the original intensity by adding Cs.

The energy spread in the electron beam was measured by using a retarding lens element built into the Faraday cup assembly. The current was measured as a function of the retarding voltage and resulting curve was then differentiated numerically. The full width at half-maximum (FWHM) of the energy distribution is taken as the energy spread after allowance is made for the resolution of the energy analyzer, which was measured to be 0.14% of the incident energy. The energy spread of the beam was thus determined to be 0.16 eV FWHM at room temperature and 0.13 eV FWHM at low temperature (110 K).

The source spin polarization was determined[4] to be 43±2% for the GaAs at 110 K. This was obtained by comparing our $S(E,\theta)$ profiles with the $P(E,\theta)$ profiles of the Rice group,[3] who used an unpolarized electron beam and measured the polarization of scattered electrons with a Mott detector. The spin polarization decreases to 36% for GaAs at room temperature.

B. The W(100) target

The tungsten crystal was 6 mm in diameter and 1.5 mm thick. We measured two different crystals which had surfaces oriented approximately 1° and $\frac{1}{4}$° from the (100) plane, respectively. The crystal was spot welded on a tungsten rod through a hole at the top edge of the crystal. A W3%Re -W25%Re thermocouple was attached on the edge of the crystal. The crystal manipulator allows X, Y, and Z translational motion, rotation of the sample to face different ports of the chamber, and tilt about an axis in the crystal surface. Azimuthal rotation about an axis normal to the surface is not possible. All the data were taken along the (010) azimuth.

The W crystal was cleaned by electron bombardment heating in 10^{-6} Torr of oxygen at 1800 K for several hours with frequent flashes to 2500 K. The oxygen was then pumped away, and the crystal was flashed to 2500 K in ultrahigh vacuum (10^{-11}-Torr range). Auger scans showed a peak ratio of C (272 eV) to W (350 eV) of less than $\frac{1}{10}$

As is well known, the W(100) surface undergoes a reconstruction. When the W temperature is higher than 400 K, the diffraction beams show a (1×1) pattern which is interpreted by previous LEED work to be an unreconstructed surface.[15] The crystal was flashed to 2500 K before each data run, and the temperature of the crystal was between 450 and 650 K while data were recorded. In this temperature range, scanning the Faraday cup through the $(\frac{1}{2},\frac{1}{2})$ beam position gave only the background intensity and no splitting of the substrate spots was observed.

C. Data acquisition

The Faraday cup collector can be moved in both the polar and azimuthal directions to measure the intensity of beams diffracted from the target crystal. Because the intensity of the electron beam incident on the crystal is not modulated, an ac component in the scattered intensity at the spin-polarization modulation frequency is solely due to spin-dependent scattering. The signal at the Faraday cup also has an average value which is the spin-averaged LEED intensity.

The electrons are transported from the photocathode to the crystal target by an electron optical system consisting of eight lens elements and four sets of deflection plates. Optimum transmission is obtained by adjusting the voltage of deflection plates and lens elements. As the crystal target is at ground potential, the beam energy is set by applying a negative voltage to the GaAs photocathode. This is done using a computer-controlled digital-to-analog converter. The beam energy is approximately 3 eV less than the nominal applied voltage due to the difference between the W(100) vacuum level and GaAs conduction band minimum.

In a typical measurement of a specular beam, the computer-controlled power supply establishes the beam energy, the signals are integrated for 1 sec, and then the power supply is set to the next beam energy. The Faraday cup current passes through a current-to-voltage converter to a lock-in amplifier which measures the spin-dependent signal. The current-to-voltage converter output is also fed to a voltmeter to obtain the spin-independent signal. Each of these outputs is digitized with a voltage-to-frequency converter and a scalar which is then read by the computer.

The computer stores the data, calculates S, displays I and S on a CRT, and provides plots as requested. Specular scattering measurements such as those displayed below in Fig. 3 are the result of 1-eV steps in beam energy and a 1-sec integration time. Thus a 100-eV scan takes about 2 min. Measurements of nonspecular beams take longer by the amount of time required for the operator to move the Faraday cup to the new beam position each time the computer sets a new incident energy. We emphasize that the spin-dependent scattering information is obtained simultaneously with the conventional spin-averaged intensity measurements without requiring any additional time.

In order to normalize the measured scattered intensity to incident beam variations, we first collect electrons with the beam aimed directly into the Faraday cup and measure the cup current versus incident electron energy. Next we move the crystal into the beam and measure the current to the crystal under the same conditions. We then calculate the ratio of the Faraday cup current to the crystal current. In all data runs the crystal current is continuously recorded by the computer as a function of beam energy. The normalized intensity profile is finally obtained by taking the dc signal collected by the Faraday cup divided by the product of the crystal current and the ratio function. This procedure corrects for variations of incident current with time or beam energy as well as for the energy dependence of the Faraday cup acceptance.

D. Determination of diffraction geometry

The normal incidence direction was found in the vertical plane by measuring the $S(E,\theta)$ profiles of the (01) and $(0\bar{1})$ beam until the peak positions and absolute magnitudes agreed with each other. The $S(E,\theta)$ profiles for the $(0\bar{1})$ and (01) beams are shown in Fig. 2. The sign of S defined in Eq. (1) is the same for each beam. Normal incidence in the horizontal plane was found by measuring $S(E,\theta)$ profiles of the horizontal spots, the $(1\bar{1})$ beam and $(1\bar{1})$ beam or the $(\bar{1}1)$ beam and the (11) beam. When a true normal incidence (both vertically and horizontally) was found, the $S(E,\theta)$ and $I(E,\theta)$ profiles of the four (11) beams agreed with each other both in peak and valley positions and in absolute magnitudes. A 0.2° change in incident angle results in an observable disagreement of the $S(E,\theta)$ profiles of the (01) and $(0\bar{1})$ beams. A laser beam reflected from a piece of polished molybdenum attached to the crystal housing enabled us to measure angle changes near normal incidence to within 0.2°.

The angle of incidence at other than normal incidence is determined by the difference between readings on the vernier attached to the arm of the Faraday cup when the cup is collecting the primary beam directly and when the cup is collecting the specularly reflected beam. The scattering angle can be read on the vernier to 0.2°. The absolute accuracy in the angle of incidence depends on the electron beam intersecting the crystal surface at the center of the Faraday cup rotation. We measured three sets of specular scattering data from two different W(100) crystal surfaces. A one-to-one correspondence between the curves in each data set was observed and the nominal angle of incidence for corresponding curves in different data sets varied by less than 2°.

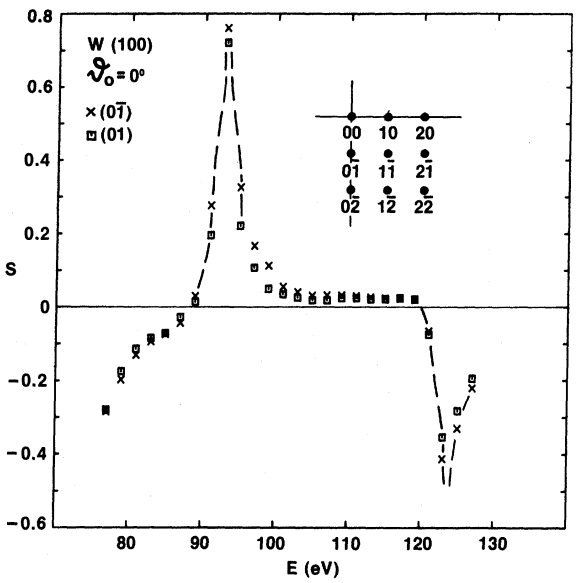

FIG. 2. $S(E,\theta)$ curves measured in 2-eV steps for the (01) and $(0\bar{1})$ beams at normal incidence are identical. The insert shows the beam labeling convention.

E. Instrument response

In order to extract the true signal from the measured signal, an accurate determination of the instrument response function is necessary.[16,17] In a typical LEED system, the following factors contribute to the finite instrument response function: (a) the energy spread of the electron beam (smaller for the GaAs electron gun than for a thermionic emitter), (b) the source extension, (c) the beam diameter (≤ 1 mm), and (d) the collector aperture size. In our instrument the response is limited by the last factor. The collector aperture is of diameter $d = 1$ mm and is located at a radius $R = 19.4$ mm from the crystal. This causes an uncertainty in reciprocal space for an incident beam normal to the surface

of

$$|\Delta\vec{K}_{\parallel}| = 2\pi(E/150)^{1/2}(d/R)\cos\vartheta \ , \qquad (4)$$

where ϑ is the diffraction angle and $\vec{K}_{\parallel}$ is the parallel momentum transfer.

III. RESULTS AND DISCUSSION

A. Experimental data

In this section we present data suitable for a comparison to a spin-polarized dynamical LEED calculation. We have measured the spin dependence $S(E,\theta)$ and LEED intensity $I(E,\theta)$ for a number of specular and nonspecular beams as listed in Table I.

In Fig. 3 we show the measured $S(E,\theta)$ profiles for the (00) beams measured on the W surface oriented to within $\frac{1}{4}°$ of the (100) plane. The angle of incidence varies from 9° to 24° in 1° steps. The sensitivity of S to diffraction conditions can be clearly seen in Fig. 3 as the angle of incidence is varied. The normalized intensity data for the specular curves are summarized in the three-dimensional plot of Fig. 4.

Both the $S(E,\theta)$ and normalized $I(E,\theta)$ profiles are plotted in Fig. 5 for five nonspecular beams taken at the normal incidence. The measured beams are in the lower right quadrant of the LEED screen as viewed from the crystal. In some energy ranges the S function changes from large positive values to large negative values as is seen in the (00) beam data. For the $(1\bar{2})$ and $(2\bar{2})$ beam, S has only negative values in the energy range we measured.

B. Comparison with other experimental data

As we have shown previously,[4] our $S(E,\theta)$ profiles agree very well with $P(E,\theta)$ profiles measured by the Rice group[3] for specular diffraction at angles of incidence from 10°–17°. The Rice group obtained their $P(E,\theta)$ profiles by measuring the polarization of an initially unpolarized beam after scattering using a Mott detector. In general, because of mulitple scattering, equivalence of the $S(E,\theta)$ and $P(E,\theta)$ measurements cannot be assumed. We showed[4] experimentally and theoretically that $S(E,\theta)=P(E,\theta)$ when the scattering plane is a mirror symmetry of the crystal. Recently, it has been shown[18] that for specular scattering, time reversal together with twofold rotational symmetry is also sufficient for $S(E,\theta)=P(E,\theta)$ when they are measured normal to the scattering plane.

As for the nonspecular beams, there are two $P(E,\theta)$ profiles over limited energy ranges available from Rice group, i.e., $(0\bar{1})$ and $(1\bar{1})$ beam at the normal incidence. The agreement in the magnitude of S and P is not as good as for the specular beams, presumably due to small deviations from normal incidence. Using laser reflection we constantly monitored the normal incidence and rechecked this periodically by measuring $S(E,\theta)$ for symmetric beams.

The $I(E,\theta)$ profiles of the (00) beams agree well with the data of the Rice group (if their angle of incidence is increased[19] by 1°) and with the data of Debe and King.[20] For nonspecular beams, the general features in our $(0\bar{1})$, $(0\bar{2})$, $(1\bar{1})$ beams agree with those of Debe and King. However, for the $(1\bar{2})$ beam, a -5-eV shift in energy has to be made in order to compare with the Debe and King $(\bar{2}1)$ beam profile. A slight departure from normal incidence in the horizontal plane could cause such a discrepancy. Since the $(1\bar{2})$ beam is on the opposite side of the vertical axis (010) from the $(\bar{2}1)$ beam, a 1° deviation in normal incidence will result in as much as a 4-eV difference in the higher-order diffracted beams in which the parallel momentum transfer has the opposite sign.

C. Comparison with theoretical calculations

We have compared the gross features of $S(E,\theta)$ experimentally determined for specular reflection with calculations for single-atom scattering,[21] but no correlation was seen. Theoretical PLEED $P(E,\theta)$ profiles have been calculated by Feder for the (00) beam at $\vartheta_0=11°$ and the (10) beam $\vartheta_0=0°$. We found good agreement between the (10) beam, calculated assuming a 10% top layer contraction, and our experimental $(0\bar{1})$ beam both in $S(E,\theta)$ and $I(E,\theta)$ profiles. The measured $S(E,\theta)$ is compared to the calculated curve in Fig. 6. However, for the (00) beam, which is very sensitive to the top-layer spacing, there is only qualitative agreement between the experimental data and the theoretical calculation when the same amount of contraction is assumed. Now that this set of LEED data is available,[22] more complete calculations are required in order to investigate the structure of the surface.

TABLE I. A list of the measured beams.

Beam	Azimuth ϕ(°)	Angle of incidence ϑ_0(°)	Energy (eV)
(00)	0	9° to 24° in 1° steps	47 → 147
$(0\bar{1})$	0	0	54 → 197
$(0\bar{2})$	0	0	67 → 197
$(1\bar{1})$	45	0	47 → 197
$(2\bar{2})$	45	0	143 → 197
$(1\bar{2})$	63.5	0	97 → 197

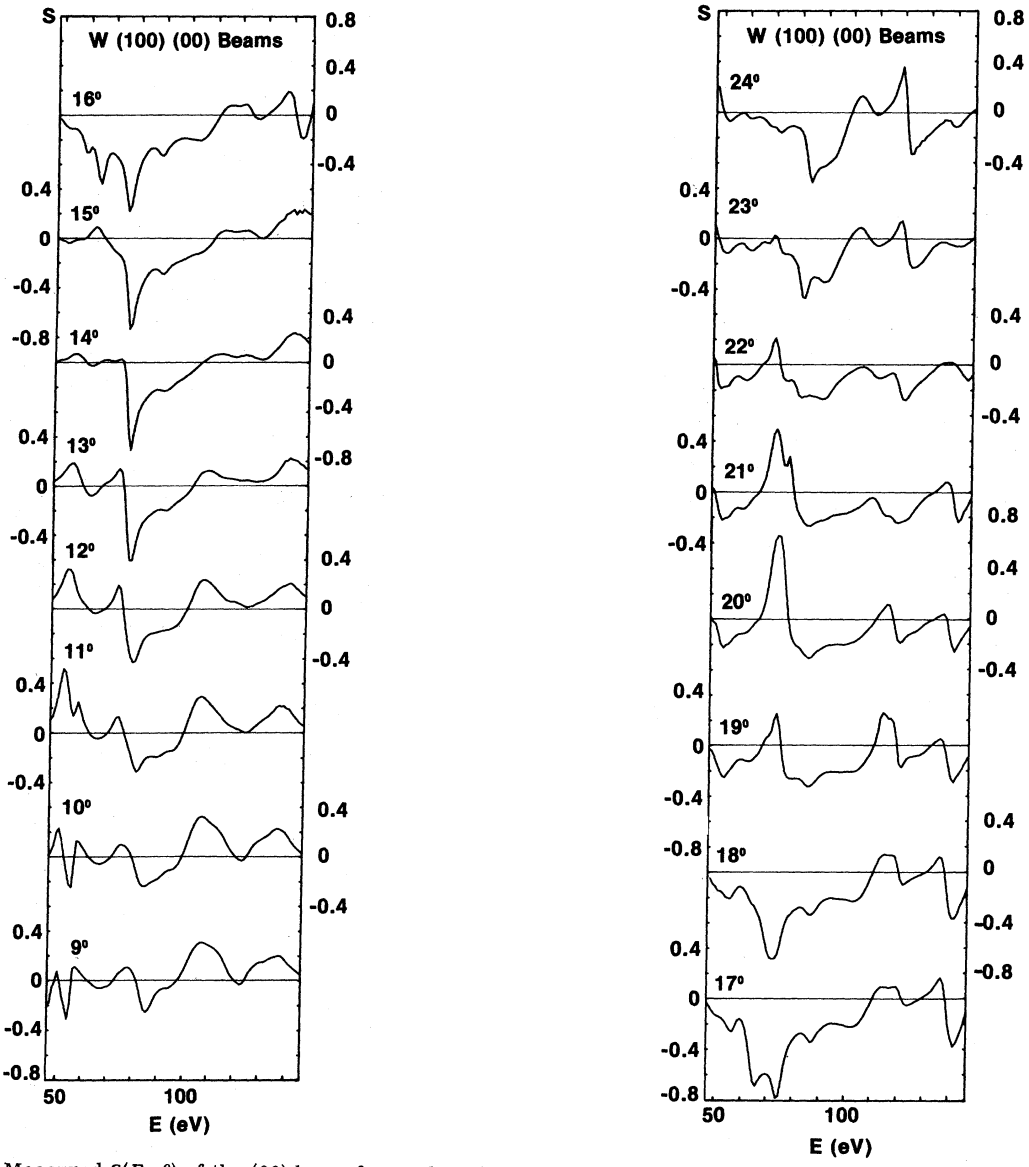

FIG. 3. Measured $S(E, \theta)$ of the (00) beam for angles of incidence from 9° to 24° in 1° steps. The scattering plane is in a (010) plane of the crystal.

IV. DEPENDENCE OF $S(E,\theta)$ ON INSTRUMENT RESPONSE

LEED dynamical calculations of the W(100) (1×1) phase and comparisons with the experimental data of different laboratories have resulted in reports[20,23–27] of top-layer contractions ranging from 4.4% to 11%. One of the reasons for the discrepancy comes from the fact that the measured $I(E, \theta)$ profiles differ depending upon the instrument used. An interesting aspect of the $S(E, \theta)$ and $P(E, \theta)$ measurements is that they are to a first approximation independent of the instrumental response. This, perhaps, partially accounts for the excellent agreement between our $S(E, \theta)$ data and the $P(E, \theta)$ data of the Rice group[3] obtained on a very different instrument.

The measured LEED intensity $I(\vec{K}_{\parallel})$ is [16] the true signal intensity $\mathcal{I}(\vec{K}_{\parallel})$ convoluted by the instrument response function $T(\vec{K}_{\parallel})$, i.e., $I(\vec{K}_{\parallel}) = \mathcal{I}(\vec{K}_{\parallel}) * T(\vec{K}_{\parallel})$. If one assumes that all angular profiles of $I(\vec{K}_{\parallel})$, $\mathcal{I}(\vec{K}_{\parallel})$, and $T(\vec{K}_{\parallel})$ are Gaussian-

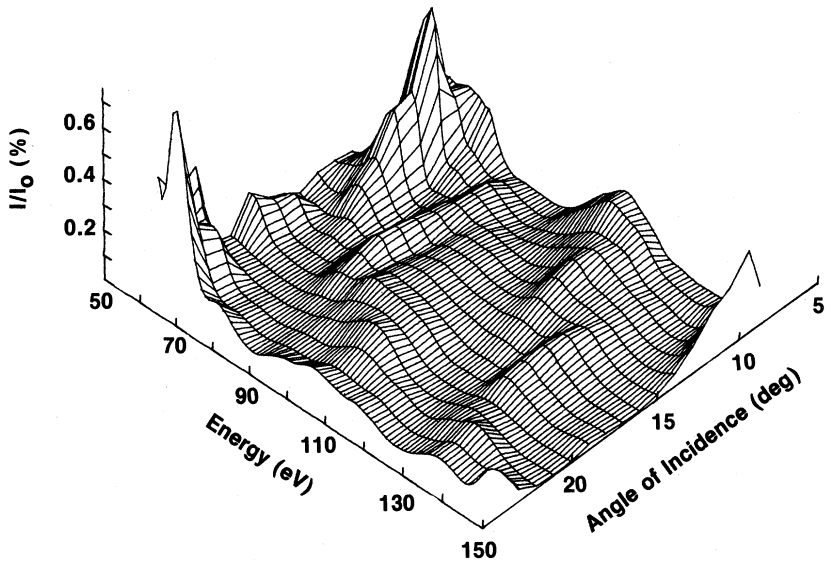

FIG. 4. Three-dimensional plot of the normalized intensity curves for specular diffraction at angles of incidence from 9° to 24°.

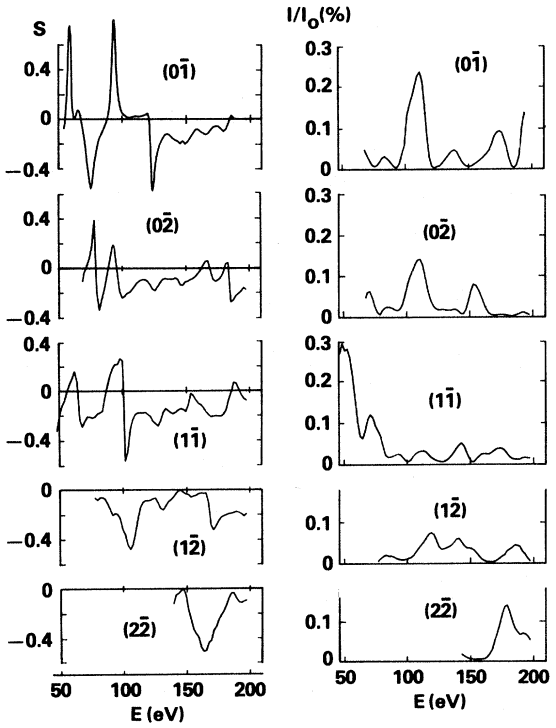

FIG. 5. Measured $S(E, \theta)$ and $I(E, \theta)$ of the nonspecular beams at the normal incidence. The intensities $I(E, \theta)$ are normalized as described in the text. Data was taken at 2 eV intervals, except for the $(0\bar{1})$ beam where higher resolution and a correction for the diffuse background was used in the region of sharp peaks in S.

like, then the full-width-at-half-maximum of the angular profile of the measured intensity, b_I, is related to the FWHM of the angular profile of the true signal intensity b_s and the FWHM of the angular profile of the instrument response function b_T by

$$b_I = (b_s^2 + b_T^2)^{1/2} \ . \tag{5}$$

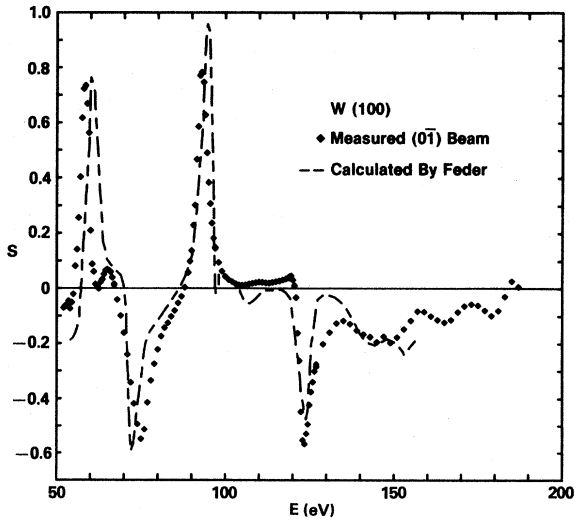

FIG. 6. Measured $S(E, \theta)$ of the $(0\bar{1})$ beam at normal incidence (♦) and Feder's calculation (from Kalisvaart *et al.*, Ref. 3) of $P(E, \theta)$ of the (10) beam assuming a 10% top-layer contraction (dashed line).

Furthermore, the peak height of a Gaussian function is inversely proportional to the FWHM for a fixed area. Thus the measured peak intensity is proportional to the true signal peak intensity and the ratio between the FWHM of the true signal intensity and the FWHM of the measured intensity,[28] i.e.,

$$I(\vec{K}_{\parallel}) = \frac{b_{\mathcal{I}}}{(b_{\mathcal{I}}^2 + b_T^2)^{1/2}} \mathcal{I}(\vec{K}_{\parallel}) = A\mathcal{I}(\vec{K}_{\parallel}) \ , \tag{6}$$

where from now on we let I and $\mathcal{I}$ correspond to peak intensities. If $b_T \neq 0$, the peak intensity recorded is reduced by the factor A. In addition to depending on the characteristics of a particular instrument, b_T also depends on the diffraction conditions; therefore A is not constant.

If we consider the $S(E, \theta)$ profile and write peak intensities $I_\uparrow$ and $I_\downarrow$ in terms of $\mathcal{I}_\uparrow$ and $\mathcal{I}_\downarrow$, Eq. (1) becomes

$$S = (1/P_0)(A\mathcal{I}_\uparrow - A'\mathcal{I}_\downarrow)/(A\mathcal{I}_\uparrow + A'\mathcal{I}_\downarrow) \ , \tag{7}$$

where the prime denotes the FWHM of the corresponsing angular profiles for antiparallel spins. Since the broadening $b_{\mathcal{I}}$ and b_T are independent of the electron beam polarization, the common factor $A = A'$ cancels. Thus, under reasonable assumptions the measured S function is faithfully representative of the true S function.

V. THE USE OF PLEED FOR SPIN ANALYSIS

The most widely used spin analyzer is the Mott detector, employing high-energy (~100 keV) electron scattering from heavy nuclei, typically a thin Au foil. The spin dependence arises from the spin-orbit interaction as the electron scatters from the nucleus rather than from the atomic core as in the case of low-energy scattering from a surface. $S(E, \theta)$ can be accurately calculated for single scattering from a nucleus.

A spin analyzer based upon PLEED has attractive features. In Mott scattering, most of the electrons go right through the thin Au foil, and those few scattered at the required large angles are dispersed over a wide angular range. In contrast, in a PLEED spin detector the electrons are coherently scattered into well defined diffraction beams. A PLEED detector can be small and avoids the experimental inconvenience of a 100-keV acceleration. On the other hand, $S(E, \theta)$ cannot be calculated sufficiently accurately for a PLEED detector so an independent calibration is required. Such a PLEED detector was recently demonstrated by Kirschner and Feder.[5] After determining S in a double scattering calibration experiment, the difference in the scattered intensity in the (20) and ($\bar{2}0$) beams at 105 at eV was used to measure the polarization of the incident beam.

At some diffraction conditions PLEED is very sensitive to small changes in scattering angle as has been vividly demonstrated in measurements on Au(110) by Müller and co-workers.[6] [It should be noted, however, that the Mott detector is also very sensitive to scattering geometry; $S(E, \theta)$ changes slowly with angle, but small changes in beam position on the Au foil cause significant changes in the solid angles accepted by the detectors leading to large spurious asymmetries in the measurement.] A knowledge of the angular sensitivity is important for a PLEED detector so one can determine the angular divergence of the beam that can be tolerated at the crystal.

An electron optical device such as a spin detector is characterized by the invariant phase-space product $EA\Omega$, where E is the energy, A is the area, and Ω is the solid angle subtended by the beam accepted by the device. If the acceptance phase-space product of the detector $(EA\Omega)_d$ is less than the phase space of the incident beam $(EA\Omega)_i$, the fraction of electrons which can be spin analyzed is $(EA\Omega)_d/(EA\Omega)_i$. Also, the efficiency of a spin analyzer is characterized by the figure of merit $S^2 I_s/I_0$, where if two beams are simultaneously monitored, $I_s = 2I$.

In making PLEED measurements of W(100) we were alert to diffraction conditions for which $S^2 I_s/I_0$ was large and not too sensitive to small angle changes. We found both a relatively high S and I_s/I_0 for the ($1\bar{1}$) beam at 70 eV, just below the 75-eV maximum in I_s/I_0 as shown in Fig. 5. The sensitivity of S to angle is shown in Fig. 7 for departures from normal incidence of ±1° and ±2°. At 70 eV, S varies from 0.21 to 0.26 for ±2° off normal. Using an average S of 0.23 and I_s/I_0 of 2.2×10^{-3} we obtain $S^2 I_s/I_0 = 1.2 \times 10^{-4}$.

In Fig. 7 we show similar measurements of the sensitivity of the ($0\bar{2}$) beam in the region around 105 eV, which was selected by Kirschner and Feder for their detector. At 105 eV, S varies from 0.13 to 0.21 for ±2° off normal and from 0.17 to 0.21 for ±1° off normal. Allowing an acceptance of ±1°, we find an average S of 0.19 and average I_s/I_0 of 2.2×10^{-3}, giving $S^2 I_s/I_0 = 8.0 \times 10^{-5}$. The choice of Kirschner and Feder[5] was based on a PLEED calculation rather than an experimental survey such as we have made; the prediction based on the calculation was very good.

The figures of merit calculated above can be compared to a typical Mott detector[29] using an Au foil, where $S = 0.25$ and $I_s/I_0 \lesssim 10^{-4}$, giving $S^2 I_s/I_0 \lesssim 6.3 \times 10^{-6}$. Whereas the figure of merit is generally lower for a Mott detector, we must also consider the acceptance $EA\Omega$ discussed above. A typical Mott detector might have an

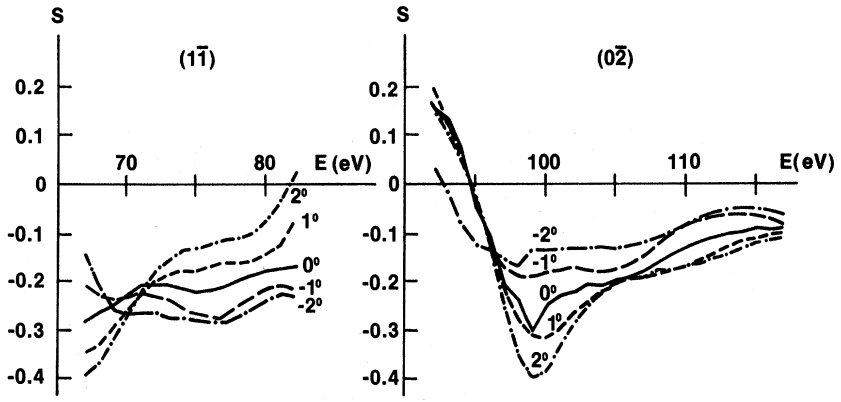

FIG. 7. S curves for the (1$\bar{1}$) and (0$\bar{2}$) nonspecular beams are shown as a function of angle of incidence ±2°, ±1°, and 0° in the energy region where $S^2 I_s/I_0$ is suitable for a polarization detector.

acceptance cone half-angle of 1° and focus the beam to a 2-mm spot at 100 keV for $EA\Omega = 300$ eV mm^2 sr. In contrast, a PLEED detector using the (1$\bar{1}$) beam with ±2° angular acceptance and a 1-mm diameter beam at 70 eV has $EA\Omega = 0.21$ eV mm^2 sr. A detector using the (0$\bar{2}$) beam with a ±1° angular acceptance at 105 eV would have $EA\Omega = 0.08$ eV mm^2 sr.

The high energy of the Mott detector, while experimentally inconvenient, greatly increases its acceptance. For experiments such as spin-polarized photoemission in a longitudinal magnetic field which causes a very large emittance,[29] a Mott detector is advantageous. On the other hand, a PLEED spin detector has the advantage when the phase space of the beam is such that the PLEED detector can accept the whole beam. Because the W(100) surface is readily contaminated by absorbed gases and reconstructs below room temperature, a more stable crystal surface is desirable. Other crystal surfaces are being tested for their suitability for a PLEED spin analyzer.

VI. SUMMARY

Using the GaAs spin-polarized electron source, we have obtained spin-dependent scattering data and LEED intensity data for the W(100) surface. Comparison with a dynamical polarized LEED calculation will test the usefulness of spin-dependent scattering measurements for the determination of surface structure. Because the measured spin-dependent quantity S is normalized to the scattered intensity, it is to first order independent of the instrument response, an obvious advantage in comparing to calculations or data from other laboratories. A spin analyzer based on PLEED was shown, in some cases, to have advantages over Mott scattering.

ACKNOWLEDGMENTS

We would like to thank the Rice Univeristy spin-polarization group and D.A. King for providing their detailed data for comparison and M. Fink and J. Moore for providing the W atom phase shifts. We are grateful to J. Unguris, B. I. Dunlap, J. C. Hamilton, T. M. Lu, and J. Houston for helpful discussions. This work was supported in part by the Office of Naval Research.

[1] J. B. Pendry, *Low-Energy Electron Diffraction*, (Academic, New York, 1974); M. A. VanHove and S. Y. Tong, *Surface Crystallography by Low-Energy Electron Diffraction* (Springer, Berlin, 1979).

[2] D. T. Pierce and F. Meier, Phys. Rev. 13, 5484 (1976); D. T. Pierce, G.-C. Wang, and R. J. Celotta, Appl. Phys. Lett. 35, 220 (1979).

[3] M. Kalisvaart, M. R. O'Neill, T. W. Riddle, F. B. Dunning, and G. K. Walters, Phys. Rev. B 17, 1570 (1978); M. R. O'Neill, M. Kalisvaart, F. B. Dunning, and G. K. Walters, Phys. Rev. Lett. 34, 1167 (1975).

[4] G.-C. Wang, B. I. Dunlap, R. J. Celotta, and D. T. Pierce, Phys. Rev. Lett. 42, 1349 (1979).

[5] J. Kirschner and R. Feder, Phys. Rev. Lett. 42, 1008 (1979).

[6] N. Müller, D. Wolf, and R. Feder, in *Electron Diffraction 1927-1977*, edited by P. J. Dobson, J. B. Pendry, and A. J. Humphreys (Institute of Physics, London, 1978), p. 281.

[7] J. Kessler, *Polarized Electrons* (Springer, New York,

[8]M. G. Lagally, in *Surface Physics of Materials*, edited by J. M. Blakely (Academic, New York, 1975), p. 419.
[9]P. J. Jennings and B. K. Sim, Surf. Sci. 33, 1 (1972).
[10]J. S. Schilling and M. B. Webb, Phys. Rev. B 2, 1665 (1970).
[11]R. Feder, Phys. Rev. Lett. 36, 598 (1976); R. Feder, Surf. Sci. 63, 283 (1977); R. Feder, P. J. Jennings, and R. O. Jones, *ibid.* 61, 307 (1976).
[12]P. J. Jennings, Jpn. J. Appl. Phys. Suppl. 2, 661 (1974).
[13]R. Zanazzi and F. Jona, Surf. Sci. 62, 61 (1977).
[14]D. T. Pierce, R. J. Celotta, G.-C. Wang, W. N. Unertl, A. Galejs, C. E. Kuyatt, and S. R. Mielczarek, Rev. Sci. Instrum. 51, 478 (1980).
[15]M. K. Debe and D. A. King, J. Phys. C 10, L303 (1977); T. E. Felter, R. A. Barker, and P. J. Estrup, Phys. Rev. Lett. 38, 1138 (1977); R. A. Barker, P. J. Estrup, F. Jona, and P. M. Marcus, Solid State Commun. 25, 375 (1978); D. A. King and G. Thomas, Surf. Sci. 92, 201 (1980), and references therein.
[16]R. L. Park, J. E. Houston, and D. G. Schreiner, Rev. Sci. Instrum. 42, 60 (1971).
[17]M. G. Lagally, G.-C. Wang, and T.-M. Lu, Crit. Rev. Solid State Sci. 7, 233 (1978); G.-C. Wang and M. G. Lagally, Surf. Sci. 81, 69 (1979).
[18]B. I. Dunlap, Solid State Commun. 35, 141 (1980); R. Feder, Phys. Lett. 78A, 103 (1980).
[19]In the comparison of $S(E, \theta)$ and $P(E, \theta)$ of Ref. 4 the nominal angle of incidence of our curves was reduced by two degrees for best agreement with the $P(E, \theta)$ data. We label the new curves presented in this work by the angles as determined in our apparatus; therefore the 12°, 14°, 16°, and 18° curves of Fig. 3 correspond to the 11°, 13°, 15°, and 17° curves of Ref. 4.
[20]M. K. Debe and D. A. King, Surf. Sci. 68, 437 (1977).
[21]M. Fink and J. Moore provided us with the relevant phase shifts for the W atom.
[22]Complete data sets are available as plots, listings, and in machine readable form.
[23]M. A. VanHove and S. Y. Tong, Surf. Sci. 54, 91 (1975).
[24]B. W. Lee, A. Ignatiev, S. Y. Tong, and M. A. VanHove, J. Vac. Sci. Technol. 14, 291 (1977).
[25]J. Kirschner and R. Feder, Surf. Sci. 79, 176 (1979).
[26]M. N. Read and G. J. Russell, Surf. Sci. 88, 95 (1979).
[27]P. Heilmann, K. Heinz, and K. Müller, Surf. Sci. 89, 84 (1979).
[28]G.-C. Wang, T.-M. Lu, and M. G. Lagally, J. Chem. Phys. 69, 479 (1978).
[29]D. T. Pierce, C. E. Kuyatt, and R. J. Celotta, Rev. Sci. Instrum. 50, 1467 (1979).